

RESEARCH ARTICLE

# *In vivo* evaluation of the antibacterial properties of a poly- $\epsilon$ -lysine and hyaluronic acid coated intramedullary implant in a New Zealand White rabbit model

Julia L. van Agtmaal<sup>1</sup>, Sanne W. G. van Hoogstraten<sup>1</sup>, Noémie Reinert<sup>2</sup>, Cynthia Calligaro<sup>3</sup>, Rajendra Kasinath<sup>4</sup>, Claudia Zindl<sup>2</sup>, Stephan Zeiter<sup>2</sup>, Nihal Engin Vrana<sup>3</sup>, Tim J. M. Welting<sup>1</sup>, Jacobus J. C. Arts<sup>1,5\*</sup>

**1** Department of Orthopaedic Surgery, Research School CAPHRI, Maastricht, the Netherlands, **2** AO Research Institute Davos, AO Foundation, Davos, Switzerland, **3** SPARTHA Medical, Strasbourg, France, **4** DePuy Synthes Biomaterials, Warsaw, Indiana, United States of America, **5** Orthopaedic Biomechanics, Department of Biomedical Engineering, Eindhoven University of Technology, Eindhoven, the Netherlands

\* [j.arts@mumc.nl](mailto:j.arts@mumc.nl)



**OPEN ACCESS**

**Citation:** van Agtmaal JL, van Hoogstraten SWG, Reinert N, Calligaro C, Kasinath R, Zindl C, et al. (2026) *In vivo* evaluation of the antibacterial properties of a poly- $\epsilon$ -lysine and hyaluronic acid coated intramedullary implant in a New Zealand White rabbit model. PLoS One 21(3): e0343597. <https://doi.org/10.1371/journal.pone.0343597>

**Editor:** Abbas Farmany, Hamadan University of Medical Sciences, IRAN, ISLAMIC REPUBLIC OF

**Received:** July 9, 2025

**Accepted:** February 9, 2026

**Published:** March 4, 2026

**Copyright:** © 2026 van Agtmaal et al. This is an open access article distributed under the terms of the [Creative Commons Attribution License](https://creativecommons.org/licenses/by/4.0/), which permits unrestricted use, distribution, and reproduction in any medium, provided the original author and source are credited.

**Data availability statement:** All relevant data are within the paper and its [Supporting Information](#) files.

## Abstract

Peri-prosthetic joint infection (PJI) is a severe complication that can arise following joint replacement surgery. PJI treatment is extremely complex due to the formation of bacterial biofilms and the emergence of antimicrobial resistance (AMR) to antibiotic classes commonly used in the treatment of PJI. This critical development highlights the urgent need for novel prophylactic strategies that do not rely on conventional antibiotic agents to prevent bacterial adherence and subsequent biofilm formation on implant surfaces. This study evaluated the contact-killing properties of a supra-molecular poly-epsilon-lysine and hyaluronic acid (PEL-10/HA-1) coating on an intramedullary nail in a New Zealand White (NZW) rabbit model. Fifteen female NZW rabbits were inoculated with *Staphylococcus aureus* (JAR 060131,  $5.9 \times 10^4$  CFU in 100  $\mu$ L PBS) in the right humerus. Seven received an uncoated nail, while eight received a PEL-10/HA-1 coated titanium alloy nail. After 7 days, the rabbits were euthanized for microbiological analysis of the nail and surrounding tissues. Remarkably, microbiological analysis showed that 4/8 of the rabbits with a coated nail had 0 CFU on the nail, versus 1/8 of the rabbits with an uncoated nail. The rinsing solution, soft tissue, and bone samples from the rabbits with a coated nail were more often culture-negative than the samples from rabbits with an uncoated nail. However, no statistically significant differences were observed between the CFUs of the coated and uncoated groups. There were no statistically significant differences between the coated and uncoated groups in other infection indicators, including white blood cell count, C-reactive protein, and plasma protein electrophoresis. While the PEL-10/HA-1 coating had a bacteriostatic and bactericidal effect *in vitro*, this effect did not translate to *in vivo*, highlighting a translational gap. The PEL-10/HA-1 coating must

**Funding:** This publication is part of the EMILIO project (with project number LSHM21057), co-funded by the PPP Allowance made available by Health-Holland, Top Sector Life Sciences & Health. This publication is also part of the DARTBAC project (with project number NWA.1292.19.354) of the research program NWA-ORC, which is (partly) financed by the Dutch Research Council (NWO). This work is supported by the EIC Accelerator SPARTHACUS (Grant No: 190184905) project (SPARTHA Medical). The funders had no role in study design, data collection and analysis, decision to publish, or preparation of the manuscript.

**Competing interests:** The authors declare no conflicts of interest. NE Vrana: Shareholder of SPARTHA Medical, C Calligaro: Employee of SPARTHA Medical. SPARTHA Medical was not involved in study design or analysis. This does not alter our adherence to PLOS ONE policies on sharing data and materials.

be optimized to enhance its antimicrobial effect, ensuring the same promising *in vivo* effect as previously observed *in vitro*.

## Introduction

Peri-prosthetic joint infection (PJI) is a severe complication that can arise following primary and revision joint replacement surgery, affecting implant survival, as well as the patient's functional outcomes and quality of life [1,2]. PJI poses a substantial burden on healthcare systems, as it is one of the leading causes of implant revision surgeries and often requires a complex treatment strategy and prolonged hospitalization [3,4]. The primary pathogens responsible for PJI are the gram-positive *Staphylococcus aureus* (*S. aureus*) and *Staphylococcus epidermidis*, and the gram-negative *Escherichia coli* (*E. coli*) and *Pseudomonas aeruginosa*, which can form a biofilm on implant surfaces [5,6]. Biofilms are complex communities of bacteria embedded in a self-produced extracellular matrix, acting as a protective barrier against the host immune response and antibiotic treatment [7]. Biofilm formation is a major cause of chronic infections, as bacteria within the biofilm can exhibit low metabolic activity, making them less susceptible to antibiotics and the immune system, contributing to persistent and difficult-to-treat infections [8]. Studies have shown a fivefold higher mortality rate for patients with PJI compared to those who had undergone an uninfected joint replacement, underscoring the severity of these infections [9,10]. The emergence of antimicrobial resistance (AMR) to antibiotic classes commonly used in PJI further complicates PJI treatment [11]. AMR poses a global health threat, as a recent study estimated that there will be 1.91 million annual deaths directly attributable to AMR in 2050 [12]. This alarming trend underscores the urgent need for novel treatment strategies that do not rely solely on antibiotics to prevent biofilm formation on implant surfaces.

A novel polyelectrolyte-based supramolecular antimicrobial contact-killing coating has been developed to prevent bacterial adhesion. Poly-epsilon-lysine (PEL-10), a polycation, has shown strong antimicrobial properties by disrupting bacterial cell membrane peptidoglycans and lipopolysaccharides, and hyaluronic acid (HA-1), a biocompatible polysaccharide, has antifouling properties that reduce bacterial attachment and promote tissue integration [13,14]. Together, these materials can form a thin coating that can potentially prevent bacterial colonization on implant surfaces. Previous studies have shown significant antibacterial properties, up to a 5-log reduction in colony-forming units (CFU) against *S. aureus* and *E. coli*, and biocompatibility of the PEL/HA coating *in vitro* [15]. An important next step toward the clinical application of the coating is to assess its antibacterial efficacy in an *in vivo* setting. This study aimed to determine the contact-killing properties of the coating on an intramedullary (IM) nail in an *in vivo* New Zealand White (NZW) rabbit model, a well-established preclinical model for studying infection prevention in orthopedic surgery [16–19]. The PEL-10/HA-1 coating has strong contact-killing properties *in vitro*, so it is expected to prevent bacterial adherence to the implant *in vivo* [15]. This study

aimed to assess the potential of this novel contact-killing PEL-10/HA-1 coating to reduce bacterial adhesion and thereby biofilm formation on orthopedic implants.

## Methods

### Institutional animal care and ethical approval

Fifteen healthy (based on clinical examination, hematocrit (Hct), and white blood cell count (WBC)) female New Zealand White (NZW) rabbits (Charles River, Sulzfeld, Germany), at the age of 22–36 weeks, with a weight of 3.0–4.5 kg, were included in the study. As treatment success in PJI is not known to differ between the sexes, only female rabbits were chosen, as they are known to fight less than males [20–22]. The rabbits were specific, opportunistic pathogen-free, and Vendor-Assured Free/Plus (SPOF and VAF/Plus). The Canton Grisons, Switzerland Ethical Committee approved this study (ethical approval number 13/2024). All experiments were conducted in accordance with Switzerland's animal protection laws and regulations. The rabbits were housed, and the surgeries were performed, in a preclinical facility accredited by the Association for Assessment and Accreditation of Laboratory Animal Care (AAALAC). The rabbits were acclimatized and housed in groups for at least 4 weeks before the surgical procedure. Throughout the experiment, the rabbits had food and water ad libitum. The NZW rabbit model for PJI was performed according to the ARRIVE guidelines, a checklist of recommendations for the complete and transparent reporting of research involving animals, and elaborated checklists [16,23]. The humerus was chosen for implantation because it is exposed to lower forces during weight-bearing, especially compared to bones in the pelvic limbs, which lowers the risk of bone fractures, nail displacement, and discomfort for the animal [16].

### Implants and coating

Medical-grade titanium 7%-aluminum 6%-niobium (TAN, ISO 5832/11) IM nails (54 mm long, 2.5 mm diameter) were manufactured at the AO Research Institute (RISystem AG, Davos, Switzerland). Test nails (n=8) were coated with PEL-10/HA-1 (SPARTHA Medical, Strasbourg, France). Before coating, the nails were sonicated for 5 min in 70% ethanol and dried at room temperature. PEL solution was prepared at 10 mg/mL (PEL-10), and HA solution was prepared at 1 mg/mL (HA-1) in Tris buffer (20 mM) at pH 7.4. The nails were dipped in the PEL-10 solution, ultrasonicated for 15 sec, rinsed in the Tris buffer, dipped in the HA-1 solution, ultrasonicated again for 15 sec, and rinsed again in the Tris buffer. This process was repeated until 36 bilayers, each consisting of a layer of PEL-10 and a layer of HA-1, were obtained, creating a thin coating (0.5–2.5  $\mu\text{m}$  range) based on the electrostatic interaction between the positively charged PEL-10 and the negatively charged HA-1. Coating adhesion to the nail was confirmed by confocal microscopy (S1 Fig). The nails were dried at room temperature and sterilized with UV light for 30 minutes. Before implantation, each nail was packaged individually and autoclaved at 143°C for 8 minutes.

### Bacterial strain

*S. aureus* JAR 060131 (Swiss Culture Collection CCOS 890, Basel, Switzerland), isolated from a patient with an infected hip prosthesis, was used in this study. A previously determined antibiotic susceptibility profile showed JAR 060131 was susceptible to all antibiotics except penicillin [24]. For each rabbit, an individual inoculum was prepared at a target concentration of  $5.9 \pm 1.3 \times 10^4$  CFU in 100  $\mu\text{L}$  of phosphate-buffered saline (PBS, P4417-50TAB, Sigma-Aldrich), based on previous studies [17–19]. The day before the surgery, JAR 060131 was inoculated from a frozen stock (stored at  $-80^\circ\text{C}$ ) into 5 mL Tryptic Soy Broth (TSB; CM0129B, Thermo Fisher Scientific) and incubated for 12–24 h at  $37^\circ\text{C}$  and 100 rpm. On the day of the surgery, 100  $\mu\text{L}$  of the overnight culture was added to 5 mL of pre-warmed TSB and incubated for 2–2.5 h at  $37^\circ\text{C}$  and 100 rpm to ensure the bacteria were in their log phase. Two hours before the surgery, the subcultures were centrifuged (7 min, 3220 RCF, RT) and washed twice in PBS. These suspensions were sonicated in a Bandelin Ultrasonic water bath (Model RK 510 H) for 1–3 min, and optical density at 600 nm ( $\text{OD}_{600}$ ) was measured using the

spectrophotometer (Multiskan GO, Thermo Scientific, SOP PRI045). A final inoculum suspension was prepared by diluting the bacterial culture to an  $OD_{600}$  of 0.25, calculated for a 1 mL volume. Bacterial concentrations were quantified by plating serial dilutions of the suspension on blood agar plates (Columbia agar containing 5% defibrinated horse blood, 10025, Liofilchem) and incubating for 24 h at 37°C, after which the CFU could be counted.

### Study design

A study timeline from surgery to euthanasia is provided in Fig 1. The study population of 15 rabbits all received the bacterial inoculum. Eight rabbits had a TAN-coated intramedullary (IM) nail implanted, with the control group (n=7) having an uncoated IM nail implanted. The experiment was based on previously published models [17–19,25]. Animals were randomly assigned to a group. All personnel were blinded until all results were analyzed, except for the study director from the animal facility in charge of correct group allocation, and the anesthetist in charge of cross-checking and documenting the allocation of the rabbits.

### Anesthesia and surgical procedure

Each rabbit was weighed and subsequently sedated accordingly, with a combination of medetomidine (Medetor®, Virbac AG, 58407, 0.2 mg/kg IM), midazolam (Dormicum®, Roche, 44448, 0.5 mg/kg IM), and fentanyl (Sintenyf®, Sintetica, 53987, 0.005 mg/kg IM). A blood sample was drawn, and a comprehensive blood count (CBC) was performed as part of the entry test for each rabbit. General anesthesia was induced with propofol to appropriate anesthetic depth (Propofol

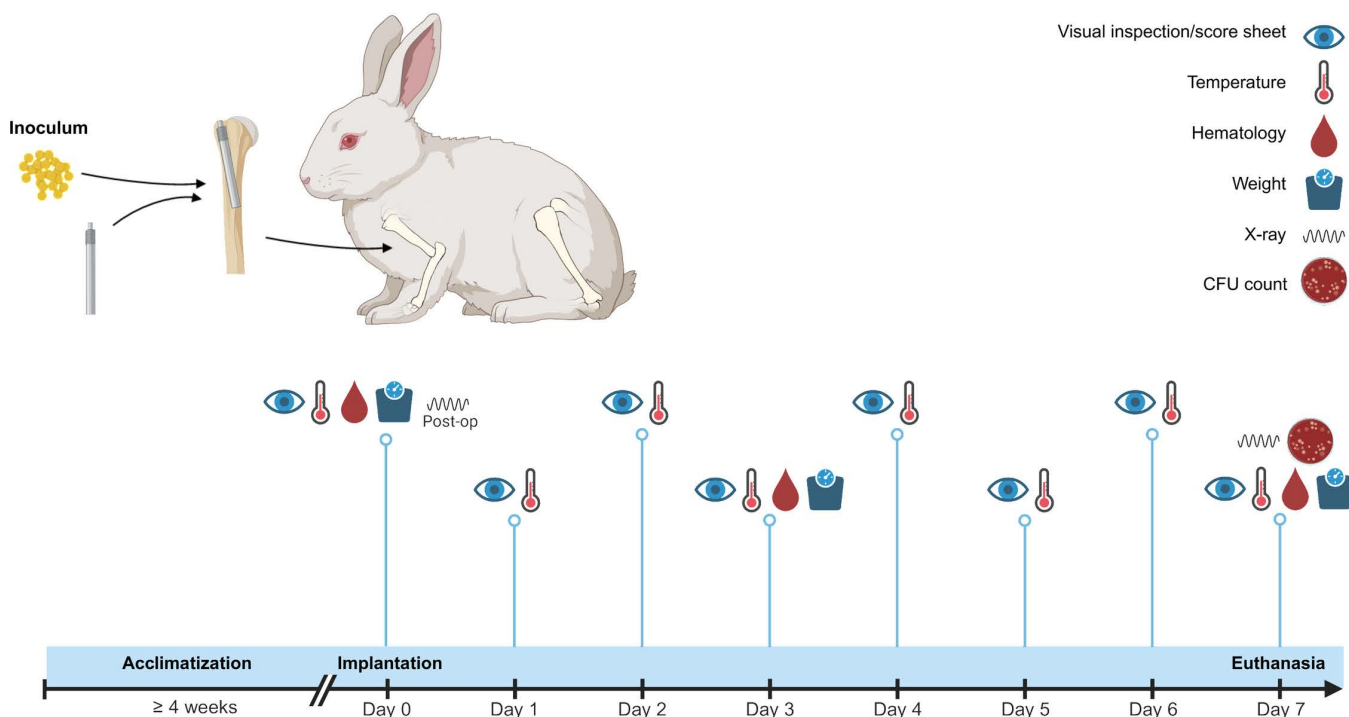


**Fig 1. Overview of the study timeline.** All rabbits were acclimatized for  $\geq 4$  weeks, after which they underwent surgery and implantation of a coated or uncoated intramedullary nail in the humerus after inoculation with  $5 \times 9 \cdot 10^4$  CFU in 100  $\mu$ L of phosphate-buffered saline. Visual inspections and temperature measurements were performed daily. Blood was drawn and weight was measured on days 0, 3, and 7. Directly after implantation and on day 7, X-rays were taken. After 7 days, the rabbits were euthanized, and bacterial cultures were made of the nail and surrounding tissues. Created in <https://BioRender.com>.

<https://doi.org/10.1371/journal.pone.0343597.g001>

1% MCT<sup>®</sup>, Fresenius, 57029, 0.2 mg/kg IV), rabbits were intubated using a cuffed endotracheal tube with an inner diameter of 3.5 mm (Rüschelit<sup>®</sup> Super Safety Clear, Ref.: 112482, Rüsch AG, Switzerland) and anesthesia was maintained using Sevoflurane (Sevoflurane Baxter<sup>®</sup>, Baxter AG, 55999, 1.8–2.2% in 0.6–0.8 L/min oxygen). Rabbits were continuously monitored during surgery using pulse oximetry, capnography, and inspiratory/expiratory anesthesia gas concentration. Carprofen (Rimadyl<sup>®</sup>, Pfizer AG, 57281, 4 mg/kg IV, 0.4 mL) was administered preoperatively and once daily for 3 consecutive days. Buprenorphine (Bupaq<sup>®</sup>, Streuli Pharma AG/63081, 0.05 mg/kg IM, 6–8h after surgery) and fentanyl (Fentanyl-Mepha<sup>®</sup>, Matrixpflaster Matrix patches, 12 µg/rabbit for 72 hours) were used as postoperative analgesia. No systemic antibiotics were administered.

The rabbits were positioned in left lateral recumbency. The right front limb was clipped, and the skin was aseptically prepared. The surgical area was draped to maintain asepsis of the surgical area. The foot was wrapped with a sterile bandage, and the leg was covered with an iodine adhesive drape (Dermadine Plus<sup>®</sup>, 20x20cm, Tiset, San Cipriano, Italy). The surgical steps are presented in [S2 Fig](#). The skin was incised over 1 cm on the lateral aspect of the proximal humerus to expose the insertion of the supraspinatus and infraspinatus tendons. The subcutaneous tissue was sharply dissected along the skin incision, and bipolar cautery was used for hemostasis. The cortex of the proximal humerus was penetrated to enter the medullary cavity just below the growth plate using a  $\varnothing$  2 mm drill bit. Using a 2.5 mm reamer, the medullary cavity was reamed to the length of the intramedullary (IM) nail so that the IM nail could be completely inserted in the medullary canal. Before inoculation and nail insertion, the depth was checked with a test nail, which was subsequently removed. All fluid was removed from the intramedullary canal using suction and an 18G intravenous catheter. The bacterial inoculum (100 µL with  $5.9 \times 10^4$  CFU) was pipetted into the IM canal, and the nail was inserted. The surgical wound was closed in three layers with absorbable suture material, consisting of myofascial and subcutaneous closure using a simple continuous pattern and skin closure using an intradermal pattern. Orthogonal radiographs of the operated humerus were taken immediately postoperatively ([Fig 2](#)) to evaluate implant positioning, and rabbits were monitored in the preparation area until fully awake, before returning them to the animal area.

### Postoperative management

During the first 3 postoperative days, rabbits were housed individually, and if animal compatibility allowed, in pairs for the remainder of the study. Rabbits were checked on the evening of the surgery and twice daily afterward, and scored using a dedicated score sheet, including observations about general demeanor, respiration, inner body temperature, third eyelid protrusion, eating and drinking behavior, defecation, soiling of fur, weight-bearing on the operated limb, paw placement, and inspection of the surgical incision ([S1 Table](#)). Bodyweight was recorded 3 and 7 days after surgery. Humane endpoints were defined as a guideline to help with decision-making for premature euthanasia in case of sudden or severe deterioration of the clinical status of the rabbits ([S1 Table](#)). Additionally, physiological measurements are needed to assess the health status, as rabbits are prey animals, and they try to hide any discomfort or illness [[22](#)]. Therefore, the initial physiological measurements of the rabbits were taken before the surgical procedure, including their weight and blood for hematological analysis. Hematological analysis was performed 3 days and 7 days after surgery, consisting of Hct, WBC, C-reactive protein (CRP), and plasma protein electrophoresis (PPEP) evaluation. Elevated WBC and CRP have been demonstrated to correlate with PJI [[16,26,27](#)]. A total rise in proteins in the plasma may indicate inflammation or infection, more specifically,  $\alpha$ - and  $\beta$ -globulins levels elevate due to acute inflammation or infection [[28,29](#)]. Hct is a standard measurement used to assess anemia, which is associated with chronic disease and may indicate osteomyelitis; however, it is not specific to this condition [[28](#)]. Hct results can be found in [S1 File](#). Seven days after surgery, rabbits were euthanized by an intravenous injection of Pentobarbital (Esconarkon<sup>®</sup>, 300 mg/mL, Streuli Tiergesundheit AG, Uznach, Switzerland). Orthogonal radiographs of the operated humerus were taken to evaluate any change in implant positioning, and a post-mortem macroscopic examination of the external body surface and surgical site was performed.

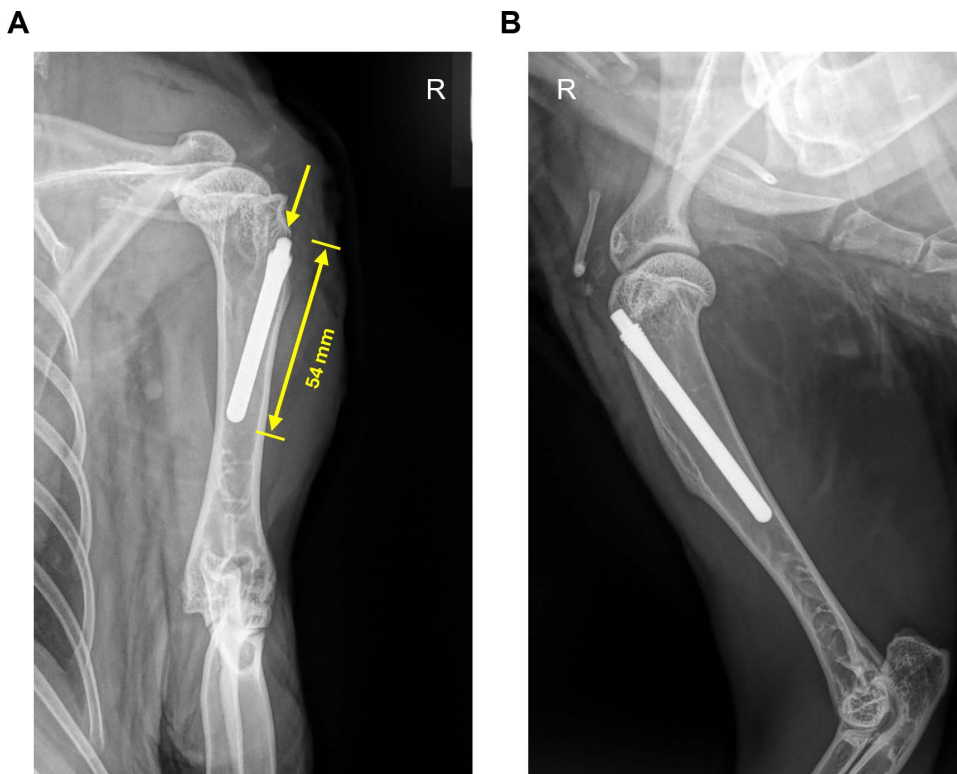


**Fig 2. Radiographs of the right humerus taken immediately postoperatively.** Craniocaudal (A), with the length of the intramedullary nail, and the insertion point indicated with the yellow arrow, and mediolateral (B).

<https://doi.org/10.1371/journal.pone.0343597.g002>

### Microbiological evaluation

After euthanasia and observation, the rabbits were positioned in left lateral recumbency, and the right front limb was excised at the scapula. The skin was wiped down with 70% ethanol and resected. The skin, radius, ulna, and scapula were resected aseptically, leaving a sterile environment for the humerus and surrounding tissue. Soft tissue was resected until the entry point of the nail was visible. For sample collection, first, soft tissue covering the nail head was resected with a sterile scalpel, and any observed abscesses were collected. This soft tissue was weighed and homogenized (Omni TH, tissue homogenizer TH-02/ TH21649) in 10 mL PBS. Next, the nail was removed from the humerus, rinsed in 15 mL PBS, transferred to a vial with 12 mL PBS, and sonicated for 3 min in a water bath. Last, the humerus was crushed using a sterile Luer bone rongeur, weighed, put into 40 mL PBS, and homogenized (Polytron System PT 3100, Kinematica Ag, Switzerland). All samples were vortexed for 5 seconds. A 200  $\mu$ L aliquot of the undiluted sample and 10  $\mu$ L aliquots from each 10-fold serial dilution of the soft tissue and bone homogenate, the rinsing solution, and the nail sonicate were added to blood agar plates. All plates were incubated at 37°C, and bacterial counts were recorded at 24h and 48h. The lower detection limit was 50 CFU/soft tissue, 75 CFU/rinsing solution, 60 CFU/nail, and 200 CFU/bone. For statistical analysis and to visualize the data on a logarithmic scale, 1 CFU per sample was assigned when no growth had occurred. From each rabbit, at least one colony was evaluated by the latex agglutination test (Staphaurex Plus, Oxoid AG) to exclude the growth of other species.

### Statistical analysis

As *in vitro*, a bacterial reduction of 3–5 log was achieved, the expected mean difference ( $\Delta$ ) was estimated at 3 (log reduction), and the standard deviation ( $\sigma$ ) for rabbits with a coated nail at 1.5 and for rabbits with an uncoated nail at 2 log,

resulting in an effect size (d) of 1.697. With a significance level of  $\alpha=0.05$  and a power of 0.9, the power calculation resulted in experimental groups of 7. The power calculation was performed using G\*Power 3.1.9.7 [30]. Statistical analysis was performed using GraphPad Prism 10.1.2 (GraphPad Software, Inc.) for Windows. The CFU from the coated and uncoated nail groups were compared per sample group with a one-sided unpaired t-test, and data were assumed to be normally distributed. 2-way ANOVA (mixed design with the between-subject factor being the uncoated or coated nail, and the within-subject factor the day of measurement) was used to compare the weight, temperature, and hematology values between the coated and uncoated nails, over time, and between rabbits. P-values <0.05 were considered statistically significant.

## Results

No humane endpoints were reached, and no rabbits were euthanized prematurely; thus, all rabbits were included in the study. The average inoculum of JAR 060131 was  $3.76 \pm 0.37 \times 10^4$  CFU (range  $3.17 \times 10^4$ – $4.40 \times 10^4$ ) in 100  $\mu$ L of PBS per rabbit, with no statistical differences between the two groups ( $p=0.4611$ ). All postoperative and post-mortem mediolateral and craniocaudal radiographs showed correct nail placement. In the uncoated group, two rabbits received an additional injection of anti-inflammatory medication on day 4 due to elevated inner body temperature; one also showed increased swelling of the surgical site on day 6. Another rabbit showed increased swelling on days 2 and 3. One rabbit exhibited increased lameness on days 5 and 6, necessitating additional opioid medication, according to the veterinarian's opinion. In the coated group, two rabbits recovered more slowly than expected from the procedure and received a subcutaneous infusion of 100 mL Ringer's lactate 1 day postoperatively. Due to continued fighting, two rabbits were separated again and housed individually on day 4.

The highest weight loss measured over 7 days was 7.7% for the coated group and 9.1% for the uncoated group, staying sufficiently below the 15% set as a humane endpoint. As shown in Fig 3, the coated group had an average weight reduction of 2.3% from baseline to day 3 and 1.7% from day 3 to day 7, while the uncoated group showed an average weight reduction of 3.1% from baseline to day 3 and 2.9% from day 3 to day 7. There was no statistical difference between the coated and uncoated groups ( $p=0.7776$ ); however, a significant difference was observed between the days

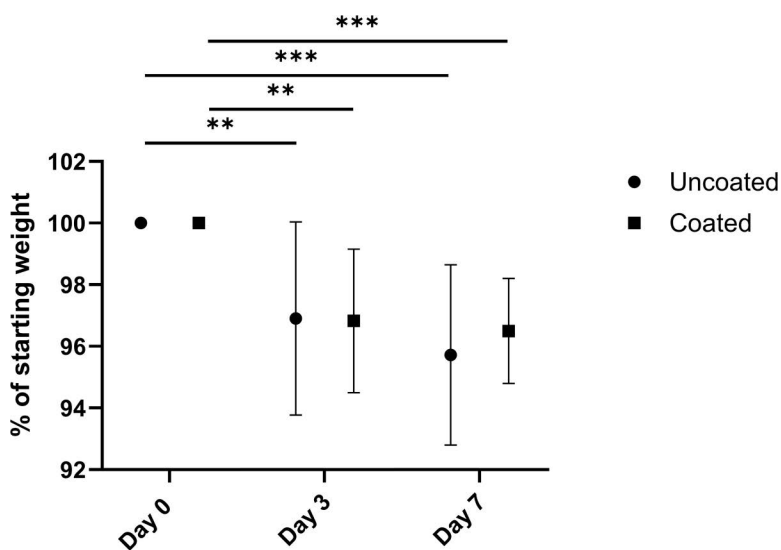


**Fig 3. Mean weight change ( $\pm$  standard deviation) throughout the experiment of the rabbits.** Presented as a percentage of the starting weight on day 0. The rabbits with uncoated and coated nails are presented in circles and squares, respectively. Statistically significant differences found by multiple comparisons are presented with \*\*  $p < 0.01$ , and \*\*\*  $p < 0.001$ .

<https://doi.org/10.1371/journal.pone.0343597.g003>



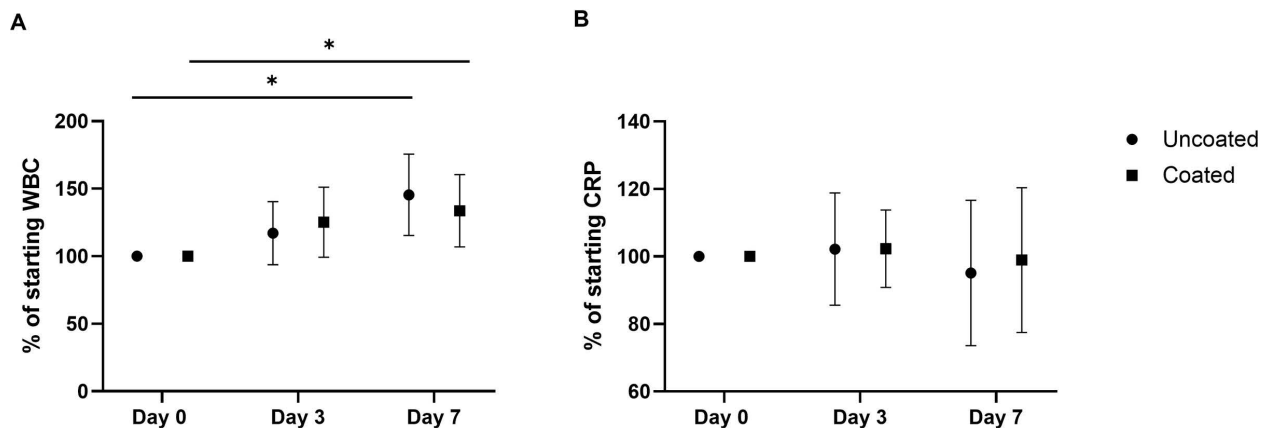


**Fig 5. Hematology parameters.** A) White blood cell count (WBC), and B) C-reactive protein (CRP) values. The mean values ( $\pm$  standard deviation) throughout the experiment of the rabbits are presented as percentages of the starting values on day 0. The rabbits with uncoated nails are presented in circles, and the coated nails in squares. Statistically significant differences found by multiple comparisons are presented with \*  $p < 0.05$ .

<https://doi.org/10.1371/journal.pone.0343597.g005>

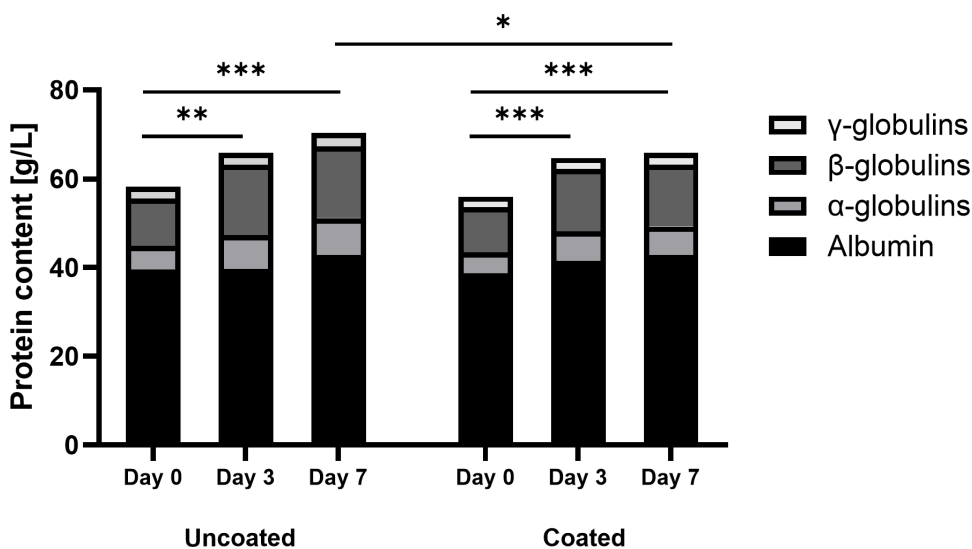


**Fig 6. The mean values of the rabbits' absolute total plasma protein electrophoresis values throughout the experiment.** Statistically significant differences found by multiple comparisons are presented with \*  $p < 0.05$ , \*\*  $p < 0.05$ , and \*\*\*  $P < 0.005$ .

<https://doi.org/10.1371/journal.pone.0343597.g006>

$\alpha$ -globulins was significantly higher ( $p = 0.0186$ ) in the uncoated group compared to the coated group and increased significantly over time ( $p < 0.0001$ ). The main effect between the uncoated and coated groups was on day 7 ( $p = 0.0137$ ). The level of  $\beta$ -globulins was significantly higher ( $p = 0.0424$ ) for the uncoated group compared to the coated group, and over the days ( $p < 0.0001$ ). The albumin level only increased significantly over the days ( $p = 0.0036$ ), but not between the two groups. The  $\gamma$ -globulins showed no significant difference between the groups or over the days. P-values of the multiple comparisons over the separate days for all measured proteins are presented in [Table 1](#). All absolute values can be found in [S5 Table](#). When the values for all proteins measured were presented as percentages of the baseline value, there was no longer a statistically significant effect between the two groups.

**Table 1. P-values of the multiple comparisons for the absolute total plasma protein electrophoresis, split per day and group. Ns=not significant ( $p > 0.05$ ). P-values between groups are in the text.**

Day	Albumin		$\alpha$ -globulins		$\beta$ -globulins		$\gamma$ -globulins		Total	
	Uncoated	Coated	Uncoated	Coated	Uncoated	Coated	Uncoated	Coated	Uncoated	Coated
0 vs. 3	ns	ns	0.0072	0.0208	0.0008	0.0068	ns	ns	0.0003	<0.0001
0 vs. 7	ns	0.0401	0.0203	0.0014	0.0276	0.0007	ns	ns	<0.0001	<0.0001
3 vs. 7	ns	ns	ns	ns	ns	ns	ns	ns	0.0338	0.7808

<https://doi.org/10.1371/journal.pone.0343597.t001>

## Discussion

PJI following primary and revision joint replacement surgery is a severe complication, affecting orthopedic implant survival, functional outcomes, and quality of life [1,2]. With the rise of AMR, the risk of therapeutic insufficiency for PJI is increasing, as many antibiotics are no longer effective in eradicating infections. Novel treatment strategies bypassing classical antibiotics are required to prevent infection and biofilm formation on the implant surface [11]. This study tested a novel PEL-10/HA-1 coating in an established NZW rabbit model for PJI. The effectiveness of a coating in reducing bacterial adhesion on implant surfaces was determined. While there were no statistically significant differences in CFU between coated and uncoated groups, a higher percentage of rabbits with coated nails had negative cultures compared to those with uncoated nails. Despite the lack of statistical significance, it was observed that no viable bacteria were recovered from four out of eight coated implants. This observed pattern suggests potential clinical relevance, warranting further investigation in larger-scale models.

Given that the PEL-10/HA-1 coating has contact-killing properties, the coating is expected to show the greatest effect on the CFU found on the nail. Four rabbits with coated nails had 0 CFU on the nail and in the rinsing solution, indicating a bactericidal effect. At the same time, four rabbits with coated nails exhibited CFU numbers near the inoculation level. This resulted in a 1.42 log mean reduction for the coated nail compared to the uncoated one, which is regarded as not clinically relevant [31]. Moreover, these results contrast with a previous *in vitro* study, demonstrating up to a 5-log CFU reduction of adherent *S. aureus* for PEL-10/HA-1 coated titanium samples compared to uncoated samples [15]. Though 50% of the coated nails remained uncontaminated, potential mechanisms for failure, such as coating degradation by serum proteins or mechanical wear, in the other cases need to be analyzed. The rinsing solution demonstrated larger differences (2.84 log) between the coated and uncoated groups. However, there was a high variation in both groups. No significant reduction was found in the CFU for the bone and soft tissue samples of the coated group compared to the uncoated group, potentially attributable to the lack of direct contact of bacteria colonizing these tissues with the coating. As the implant is near bacteria that persist in the bone and soft tissue, it is at risk of being recolonized by proliferating bacteria. Based on the current results, it cannot be concluded that the PEL-10/HA-1 coating can prevent bacterial adhesion to the implant. However, as half of the rabbits with a coated implant already showed no bacterial adhesion, this study shows the coating's potential when further optimized.

There were no significant differences between the coated and uncoated groups in other infection indicators, including weight loss, WBC, and CRP. The WBC slightly rose over the days in both groups, which may be a stress reaction to the surgery and the inoculum [16,28]. Slight weight loss in both groups after surgery was to be expected due to the opioid medication (Buprenorphine) on the day of surgery and a fentanyl patch for the first three days post-op. Previous studies with an uncontaminated implant showed that weight returned to normal after 5 weeks [32,33]. The significant elevation of total plasma protein levels (mainly due to the  $\alpha$ - and  $\beta$ -globulins) in the uncoated group compared to the coated group can be an indication of acute (bacterial) infection [28,29]. However, this elevation was no longer significant when the values were normalized to the baseline value, and should therefore be interpreted with caution. As immunoglobulins ( $\gamma$ -globulins) mainly consist of antibodies, an elevation indicates chronic inflammation [28,29]. Elevated levels of WBC, CRP, and  $\alpha$ -,  $\beta$ -

and  $\gamma$ -globulins measure inflammation. The fact that these values are not elevated for the coated group indicates that the PEL-10/HA-1 coating does not induce a statistically significant inflammatory reaction in the rabbit's body.

Translating and implementing new antimicrobial techniques remains challenging, and discrepancies between *in vitro* and *in vivo* results are commonly observed. A silver multilayer (SML) coating was previously tested *in vitro* utilizing the same ISO 22196, ASTM E2180-18, and JIS Z 2801 test combination as the PEL-10/HA-1 coating, resulting in a >3 log reduction [34]. However, when tested in a 7-day NZW rabbit model, the SML coating resulted in a decrease of 1.6 log on the nail and 1.6 log in the rinsing solution [35]. Another coating containing the antimicrobial peptide OP-145 eradicated all bacteria *in vitro*; however, in a 28-day NZW rabbit model, some rabbits developed infections exceeding the inoculum level [18]. *In vitro* findings have been shown to translate effectively to *in vivo* for a gentamicin-hydroxyapatite coating [36]. However, *in vitro* antibiotic resistance was observed, and antibiotics such as gentamicin may impair bone ingrowth around the implant [36,37]. It is unknown if these studies combined coatings with systemic antibiotics. *In vitro* test methods often lack the complexity of *in vivo* systems, and bacterial strains can react differently *in vitro* and *in vivo* [38,39].

Translating *in vitro* results to *in vivo* outcomes is difficult due to non-standardized protocols, weak correlation with clinical results, and the limited predictive reliability of current models [38]. *In vitro* test methods lack complexity and clinical relevance, but *in vivo* situations also vary between animals, and bacterial strains can respond differently *in vitro* and *in vivo* [38,39]. Several often overlooked factors *in vitro* include fluid flow [38], the impact of the immune response [40], the effect of bone marrow and blood serum proteins [41], synovial fluid [42], quorum sensing [43], and the force applied during arthroplasty surgeries [44]. Preclinical *in vivo* models are essential for studying host response, implant integration, and pathogen interaction to help bridge the translational gap to clinical applications [39]. To enhance clinical translation, *in vivo* studies should tailor their methodology and outcome parameters based on the intended use and mechanism of action of the antibacterial method [16]. Additionally, when performing a power calculation, this translational gap from *in vitro* to *in vivo* must be considered, as assuming a 3-log reduction could have resulted in an underpowered calculation for this study.

The choice of a 7-day PJI NZW rabbit model was based on previous studies, ensuring a reliable and standardized framework, suited for testing a contact-killing coating. As *S. aureus* is most prevalent in PJI in countries of the European Union, this study used a clinical methicillin-susceptible *S. aureus* strain [45]. The JAR 060131 *S. aureus* strain has previously been characterized and represents the most prevalent epidemic clones of *S. aureus* [17–19,24,25]. The inoculum levels tested in this study are substantially greater than those typically encountered in the clinical setting, creating a challenge for a coating designed for prevention rather than treatment of PJI [46]. Previous studies using the JAR 060131 strain demonstrated that the inoculum used in this study should be sufficient to create an infection in all untreated control rabbits, yet low enough to avoid inducing systemic sepsis [17–19,25,47]. However, comparable to this study, variation in the control groups in these previous studies was also high. Furthermore, how much of the bacterial suspension came into direct contact with the contact-killing coating is uncertain. Moreover, bacteria might colonize and persist better in peri-implant tissue compared to the implant surface [17,48,49]. Clinically, orthopedic infections usually manifest at lower doses than those inoculated in the rabbit model and are less localized, which cannot be modeled *in vivo* [50–52]. Although the used method of inoculation is widely applied in preclinical PJI research, it has inherent limitations in fully replicating the clinical situation, and alternative approaches (such as pre-infecting implants prior to implantation) likewise face translational challenges and introduce different sources of experimental bias [16].

Moving forward, the *in vivo* on-or-off bactericidal effect of the PEL-10/HA-1 coating needs to be optimized. The PEL-10/HA-1 coating has shown both a bacteriostatic and bactericidal effect *in vitro*. These effects are known to differ based on the concentration of the coating and the test conditions [53]. Further *in vitro* and *in vivo* studies will be needed to evaluate whether coatings with higher PEL-10/HA-1 concentrations improve antimicrobial efficacy while remaining within acceptable biocompatibility thresholds. HA-1 forms a hydrogel structure with a high hydration capacity and hydrophilicity, enhancing its antifouling properties by developing a hydration layer that eliminates binding sites for protein and bacterial adhesion [54,55]. However, the high activity of HA-1 with body fluid proteins can disrupt the hydration layer, reducing the antifouling properties [54,55]. Pre-wetting

of the coating before implantation could pre-establish the hydration layer and form a steric barrier, reducing available binding sites for proteins and retaining hydrophilicity [54]. Furthermore, several sterilization procedures should be tested to minimize the chance of potential thermally induced degradation. Since there is currently no comparable alternative commercially available to compare the PEL-10/HA-1 coating, no positive control could be used in this study. Ideally, with the emergence of AMR, alternatives to antibiotics are preferred. However, current practice still relies on combination therapy to prevent systemic infections. Thus, the contact-killing PEL-10/HA-1 coating would likely be used alongside systemic antibiotics to enhance infection control and mitigate orthopedic implant-related infection risks. A future study could therefore include control groups with a coated nail combined with antibiotics and an uncoated nail with antibiotics. For future studies, once the antibacterial efficacy of the coating has been established, osseointegration properties should also be evaluated as an outcome parameter in an *in vivo* study. Although a 7-day study duration is commonly used in NZW rabbits to assess infection progression, extending the duration to up to six weeks [56–61] is preferable in future studies to examine both the long-term antibacterial effect of the coating and its impact on the osseointegration of the implant [16]. In an extended experiment, histopathology can be used to examine in more detail the implant-host interaction, biocompatibility, inflammatory response, and bone ingrowth. Histopathology or microscopy can also be implemented to confirm the presence of a mature biofilm on the control implants.

## Conclusion

This study explored the antimicrobial activity of the PEL-10/HA-1 coating for the first time in an *in vivo* model, for further pre-clinical assessment following promising *in vitro* results. While a bacteriostatic and bactericidal effect was observed for the PEL-10/HA-1 coating *in vitro*, this effect did not fully translate to the *in vivo* situation, highlighting a translational gap. Though no significant differences were found between the uncoated and coated groups, samples from the rabbits with a coated nail were more often culture-negative than samples from the rabbits with an uncoated nail. Four out of eight rabbits had an uncontaminated coated nail, indicating a binary effect of the coating. The PEL-10/HA-1 coating will be optimized further by testing if increasing the concentration to PEL-20 and HA-5, or the addition of polyarginine, will enhance its antimicrobial effect while preserving its biocompatibility, ensuring the same promising effect *in vivo* as previously found *in vitro*. The effect on macrophage polarization will also be tested.

## Supporting information

**S1 Fig. PEL-10/HA-1 coated nails labeled with Poly-L-Lysine coupled with fluorescein isothiocyanate (PLL-FITC) (green), observed with confocal microscopy.** No fluorescence is observed under the same conditions for uncoated nails.

(TIF)

**S2 Fig. Surgical procedure.** A) view of the lateral aspect of the proximal humerus after incision of the skin and dissection of the subcutaneous tissue with the tissues retracted using a self-retaining retractor – the insertion of the supraspinatus and infraspinatus tendon are exposed; B) the medullary cavity is reamed; C) fluid is suctioned from the intramedullary canal; D) bacterial inoculation; E) insertion of the intramedullary nail.

(TIF)

**S1 File. HCT.**

(DOCX)

**S1 Table. Score sheet.**

(DOCX)

**S2 Table. Weight.**

(DOCX)

**S3 Table. Temperature.** Values outside the reference range are in bold (38.5–39.5°C).  
(DOCX)

**S4 Table. WBC, HCT, CRP.** Values outside the reference ranges are in bold: WBC = 5.5–12.5 [ $\times 10^3/\mu\text{L}$ ]; HCT = 33–50 [%].  
(DOCX)

**S5 Table. Protein electrophoresis.**  
(DOCX)

## Acknowledgments

The authors gratefully acknowledge Marco Chittò, Thomas Fintan Moriarty, and Iris Keller-Stoddart of the AO Research Institute Davos for their valuable assistance during the experimental phase.

## Author contributions

**Conceptualization:** Julia L. van Agtmaal, Nihal Engin Vrana, Jacobus J.C. Arts.

**Data curation:** Julia L. van Agtmaal.

**Formal analysis:** Julia L. van Agtmaal.

**Funding acquisition:** Nihal Engin Vrana, Jacobus J.C. Arts.

**Investigation:** Julia L. van Agtmaal, Sanne W.G. van Hoogstraten, Noémie Reinert.

**Methodology:** Julia L. van Agtmaal, Sanne W.G. van Hoogstraten, Cynthia Calligaro, Claudia Zindl, Stephan Zeiter, Nihal Engin Vrana, Jacobus J.C. Arts.

**Project administration:** Julia L. van Agtmaal, Claudia Zindl, Stephan Zeiter.

**Resources:** Cynthia Calligaro, Rajendra Kasinath, Nihal Engin Vrana.

**Supervision:** Claudia Zindl, Tim J.M. Welting, Jacobus J.C. Arts.

**Validation:** Julia L. van Agtmaal.

**Visualization:** Julia L. van Agtmaal.

**Writing – original draft:** Julia L. van Agtmaal, Sanne W.G. van Hoogstraten.

**Writing – review & editing:** Julia L. van Agtmaal, Sanne W.G. van Hoogstraten, Noémie Reinert, Cynthia Calligaro, Rajendra Kasinath, Claudia Zindl, Stephan Zeiter, Nihal Engin Vrana, Tim J.M. Welting, Jacobus J.C. Arts.

## References

- Shichman I, Sobba W, Beaton G, Polisetty T, Nguyen HB, Dipane MV, et al. The Effect of Prosthetic Joint Infection on Work Status and Quality of Life: A Multicenter, International Study. *J Arthroplasty*. 2023;38(12):2685-2690.e1. <https://doi.org/10.1016/j.arth.2023.06.015> PMID: [37353111](https://pubmed.ncbi.nlm.nih.gov/37353111/)
- Thompson O, W-Dahl A, Stefánsdóttir A. Increased short- and long-term mortality amongst patients with early periprosthetic knee joint infection. *BMC Musculoskelet Disord*. 2022;23(1):1069. <https://doi.org/10.1186/s12891-022-06024-y> PMID: [36474195](https://pubmed.ncbi.nlm.nih.gov/36474195/)
- Li C, Renz N, Trampuz A. Management of Periprosthetic Joint Infection. *Hip Pelvis*. 2018;30(3):138–46. <https://doi.org/10.5371/hp.2018.30.3.138> PMID: [30202747](https://pubmed.ncbi.nlm.nih.gov/30202747/)
- Premkumar A, Kolin DA, Farley KX, Wilson JM, McLawhorn AS, Cross MB, et al. Projected Economic Burden of Periprosthetic Joint Infection of the Hip and Knee in the United States. *J Arthroplasty*. 2021;36(5):1484-1489.e3. <https://doi.org/10.1016/j.arth.2020.12.005> PMID: [33422392](https://pubmed.ncbi.nlm.nih.gov/33422392/)
- Davidson DJ, Spratt D, Liddle AD. Implant materials and prosthetic joint infection: The battle with the biofilm. *EFORT Open Rev*. 2019; p. 633–9.
- Rodríguez-Pardo D, Pigrau C, Lora-Tamayo J, Soriano A, del Toro MD, Cobo J, et al. Gram-negative prosthetic joint infection: outcome of a debridement, antibiotics and implant retention approach. A large multicentre study. *Clin Microbiol Infect*. 2014;20(11):O911-9. <https://doi.org/10.1111/1469-0691.12649> PMID: [24766536](https://pubmed.ncbi.nlm.nih.gov/24766536/)
- Gbejuade HO, Lovering AM, Webb JC. The role of microbial biofilms in prosthetic joint infections. *Acta Orthop*. 2015;86(2):147–58. <https://doi.org/10.3109/17453674.2014.966290> PMID: [25238433](https://pubmed.ncbi.nlm.nih.gov/25238433/)

8. Bjarnsholt T. The role of bacterial biofilms in chronic infections. *APMIS Suppl.* 2013;(136):1–51. <https://doi.org/10.1111/apm.12099> PMID: [23635385](https://pubmed.ncbi.nlm.nih.gov/23635385/)
9. Xu Y, Huang TB, Schuetz MA, Choong PFM. Mortality, patient-reported outcome measures, and the health economic burden of prosthetic joint infection. *EFORT Open Rev.* 2023;8(9):690–7. <https://doi.org/10.1530/EOR-23-0078> PMID: [37655835](https://pubmed.ncbi.nlm.nih.gov/37655835/)
10. Natsuhara KM, Shelton TJ, Meehan JP, Lum ZC. Mortality During Total Hip Periprosthetic Joint Infection. *J Arthroplasty.* 2019;34(7S):S337–42. <https://doi.org/10.1016/j.arth.2018.12.024> PMID: [30642705](https://pubmed.ncbi.nlm.nih.gov/30642705/)
11. Stevoska S, Himmelbauer F, Stifflinger J, Stadler C, Pisecky L, Gotterbarm T, et al. Significant Difference in Antimicrobial Resistance of Bacteria in Septic Revision between Total Knee Arthroplasty and Total Hip Arthroplasty. *Antibiotics (Basel).* 2022;11(2):249. <https://doi.org/10.3390/antibiot-ics11020249> PMID: [35203849](https://pubmed.ncbi.nlm.nih.gov/35203849/)
12. GBD 2021 Antimicrobial Resistance Collaborators. Global burden of bacterial antimicrobial resistance 1990–2021: a systematic analysis with forecasts to 2050. *Lancet.* 2024;404(10459):1199–226. [https://doi.org/10.1016/S0140-6736\(24\)01867-1](https://doi.org/10.1016/S0140-6736(24)01867-1) PMID: [39299261](https://pubmed.ncbi.nlm.nih.gov/39299261/)
13. Lebaudy E, Guilbaud-Chéreau C, Frisch B, Vrana NE, Lavallo P. The High Potential of  $\epsilon$ -Poly-L-Lysine for the Development of Antimicrobial Biomaterials. *Adv NanoBiomed Res.* 2023;3(12). <https://doi.org/10.1002/anbr.202300080>
14. Gribova V, Boulmedais F, Dupret-Bories A, Calligaro C, Senger B, Vrana NE, et al. Polyanionic Hydrogels as Reservoirs for Polycationic Antibiotic Substitutes Providing Prolonged Antibacterial Activity. *ACS Appl Mater Interfaces.* 2020;12(17):19258–67. <https://doi.org/10.1021/acsami.9b23140> PMID: [32292035](https://pubmed.ncbi.nlm.nih.gov/32292035/)
15. van Agtmaal JL, Gielen AMC, van Hoogstraten SWG, Peeters LCW, Akkache A, Kasinath R, et al. In vitro assessment of antibacterial and biocompatibility properties of a poly- $\epsilon$ -lysine and hyaluronic acid contact-killing coating to prevent prosthetic joint infection. *PLoS One.* 2026;21(1):e0340632. <https://doi.org/10.1371/journal.pone.0340632> PMID: [41615966](https://pubmed.ncbi.nlm.nih.gov/41615966/)
16. van Agtmaal JL, van Hoogstraten SWG, Arts JJC. Prosthetic Joint Infection Research Models in NZW Rabbits: Opportunities for Standardization-A Systematic Review. *J Funct Biomater.* 2024;15(10).
17. Moriarty TF, Campoccia D, Nees SK, Boure LP, Richards RG. In vivo evaluation of the effect of intramedullary nail microtopography on the development of local infection in rabbits. *Int J Artif Organs.* 2010;33(9):667–75. <https://doi.org/10.1177/039139881003300913> PMID: [20890880](https://pubmed.ncbi.nlm.nih.gov/20890880/)
18. de Breij A, Riool M, Kwakman PHS, de Boer L, Cordfunke RA, Drijfhout JW, et al. Prevention of Staphylococcus aureus biomaterial-associated infections using a polymer-lipid coating containing the antimicrobial peptide OP-145. *J Control Release.* 2016;222:1–8. <https://doi.org/10.1016/j.jconrel.2015.12.003> PMID: [26658071](https://pubmed.ncbi.nlm.nih.gov/26658071/)
19. Metsemakers W-J, Emanuel N, Cohen O, Reichart M, Potapova I, Schmid T, et al. A doxycycline-loaded polymer-lipid encapsulation matrix coating for the prevention of implant-related osteomyelitis due to doxycycline-resistant methicillin-resistant Staphylococcus aureus. *J Control Release.* 2015;209:47–56. <https://doi.org/10.1016/j.jconrel.2015.04.022> PMID: [25910578](https://pubmed.ncbi.nlm.nih.gov/25910578/)
20. Mironenko CM, Kapadia M, Donlin L, Figgie M, Carli AV, Henry M. Sex differences in prosthetic joint infection. *Open Forum Infectious Diseases.* Oxford University Press; 2021.
21. Thurston S, Burlingame L, Lester PA, Lofgren J. Methods of Pairing and Pair Maintenance of New Zealand White Rabbits (*Oryctolagus Cuniculus*) Via Behavioral Ethogram, Monitoring, and Interventions. *J Vis Exp.* 2018;(133):57267. <https://doi.org/10.3791/57267> PMID: [29608160](https://pubmed.ncbi.nlm.nih.gov/29608160/)
22. Mapara M, Thomas BS, Bhat KM. Rabbit as an animal model for experimental research. *Dent Res J (Isfahan).* 2012;9(1):111–8. <https://doi.org/10.4103/1735-3327.92960> PMID: [22363373](https://pubmed.ncbi.nlm.nih.gov/22363373/)
23. ARRIVE guidelines London, England: National Centre for the Replacement Refinement & Reduction of Animals in Research; 2024. Available from: <https://arriveguidelines.org/>
24. Campoccia D, Montanaro L, Moriarty TF, Richards RG, Ravaioli S, Arciola CR. The selection of appropriate bacterial strains in preclinical evaluation of infection-resistant biomaterials. *Int J Artif Organs.* 2008;31(9):841–7. <https://doi.org/10.1177/039139880803100913> PMID: [18924097](https://pubmed.ncbi.nlm.nih.gov/18924097/)
25. Moriarty TF, Debeve L, Boure L, Campoccia D, Schlegel U, Richards RG. Influence of material and microtopography on the development of local infection in vivo: experimental investigation in rabbits. *Int J Artif Organs.* 2009;32(9):663–70. <https://doi.org/10.1177/039139880903200916> PMID: [19882548](https://pubmed.ncbi.nlm.nih.gov/19882548/)
26. Vaishya R, Sardana R, Butta H, Mendiratta L. Laboratory diagnosis of Prosthetic Joint Infections: Current concepts and present status. *J Clin Orthop Trauma.* 2019;10(3):560–5. <https://doi.org/10.1016/j.jcot.2018.10.006> PMID: [31061590](https://pubmed.ncbi.nlm.nih.gov/31061590/)
27. Barbari E, Mabry T, Tsaras G, Spangehl M, Erwin PJ, Murad MH, et al. Inflammatory blood laboratory levels as markers of prosthetic joint infection: a systematic review and meta-analysis. *J Bone Joint Surg Am.* 2010;92(11):2102–9. <https://doi.org/10.2106/JBJS.I.01199> PMID: [20810860](https://pubmed.ncbi.nlm.nih.gov/20810860/)
28. Melillo A. Rabbit Clinical Pathology. *J Exot Pet Med.* 2007;16(3):135–45. <https://doi.org/10.1053/j.jepm.2007.06.002> PMID: [32362792](https://pubmed.ncbi.nlm.nih.gov/32362792/)
29. Melillo A. Applications of serum protein electrophoresis in exotic pet medicine. *Vet Clin North Am Exot Anim Pract.* 2013;16(1):211–25. <https://doi.org/10.1016/j.cvex.2012.11.002> PMID: [23347545](https://pubmed.ncbi.nlm.nih.gov/23347545/)
30. Faul F, Erdfelder E, Lang A-G, Buchner A. G\*Power 3: a flexible statistical power analysis program for the social, behavioral, and biomedical sciences. *Behav Res Methods.* 2007;39(2):175–91. <https://doi.org/10.3758/bf03193146> PMID: [17695343](https://pubmed.ncbi.nlm.nih.gov/17695343/)
31. Rumbaugh KP. How well are we translating biofilm research from bench-side to bedside? *Biofilm.* 2020;2:100028. <https://doi.org/10.1016/j.bio-film.2020.100028> PMID: [33447813](https://pubmed.ncbi.nlm.nih.gov/33447813/)
32. Odekerken JCE, Arts JJC, Surtel DAM, Walenkamp GHIM, Welting TJM. A rabbit osteomyelitis model for the longitudinal assessment of early post-operative implant infections. *J Orthop Surg Res.* 2013;8:38. <https://doi.org/10.1186/1749-799X-8-38> PMID: [24188807](https://pubmed.ncbi.nlm.nih.gov/24188807/)

33. Odekerken JCE, Brans BT, Welting TJM, Walenkamp GHIM. (18)F-FDG microPET imaging differentiates between septic and aseptic wound healing after orthopedic implant placement: a longitudinal study of an implant osteomyelitis in the rabbit tibia. *Acta Orthop*. 2014;85(3):305–13. <https://doi.org/10.3109/17453674.2014.900894> PMID: 24673540
34. van Hoogstraten SWG, Fechter J, Bargon R, van Agtmaal JL, Peeters LCW, Geurts J, et al. The Antibacterial Properties of a Silver Multilayer Coating for the Prevention of Bacterial Biofilm Formation on Orthopedic Implants—An In Vitro Study. *Coatings*. 2024;14(2):216. <https://doi.org/10.3390/coatings14020216>
35. Fabritius M, Al-Munajjed AA, Freytag C, Jülke H, Zehe M, Lemarchand T, et al. Antimicrobial Silver Multilayer Coating for Prevention of Bacterial Colonization of Orthopedic Implants. *Materials (Basel)*. 2020;13(6):1415. <https://doi.org/10.3390/ma13061415> PMID: 32245004
36. Neut D, Dijkstra RJ, Thompson JI, Kavanagh C, van der Mei HC, Busscher HJ. A biodegradable gentamicin-hydroxyapatite-coating for infection prophylaxis in cementless hip prostheses. *Eur Cell Mater*. 2015;29:42–55; discussion 55–6. <https://doi.org/10.22203/ecm.v029a04> PMID: 25552428
37. Rathbone CR, Cross JD, Brown KV, Murray CK, Wenke JC. Effect of various concentrations of antibiotics on osteogenic cell viability and activity. *J Orthop Res*. 2011;29(7):1070–4. <https://doi.org/10.1002/jor.21343> PMID: 21567453
38. Moriarty TF, Grainger DW, Richards RG. Challenges in linking preclinical anti-microbial research strategies with clinical outcomes for device-associated infections. *Eur Cell Mater*. 2014;28:112–28; discussion 128. <https://doi.org/10.22203/ecm.v028a09> PMID: 25214018
39. Moriarty TF, Harris LG, Mooney RA, Wenke JC, Riool M, Zaat SAJ, et al. Recommendations for design and conduct of preclinical in vivo studies of orthopedic device-related infection. *J Orthop Res*. 2019;37(2):271–87. <https://doi.org/10.1002/jor.24230> PMID: 30667561
40. Berti A, Rose W, Nizet V, Sakoulas G, editors. *Antibiotics and innate immunity: a cooperative effort toward the successful treatment of infections*. Open Forum Infectious Diseases. Oxford University Press US; 2020.
41. Beer J, Wagner CC, Zeitlinger M. Protein binding of antimicrobials: methods for quantification and for investigation of its impact on bacterial killing. *AAPS J*. 2009;11(1):1–12. <https://doi.org/10.1208/s12248-008-9072-1> PMID: 19117135
42. De Bleecckere A, van Charante F, Debord T, Vandendriessche S, De Cock M, Verstraete M, et al. A novel synthetic synovial fluid model for investigating biofilm formation and antibiotic susceptibility in prosthetic joint infections. *Microbiol Spectr*. 2025;13(1):e0198024. <https://doi.org/10.1128/spectrum.01980-24> PMID: 39612218
43. Bevers R, Voort M, Loo I, Geurts J, Arts J. The Role of Material Technologies Targeting *P. Aeruginosa* and *S. Aureus* Quorum Sensing in Biofilm Formation. *MRAJ*. 2022;10(10). <https://doi.org/10.18103/mra.v10i10.3007>
44. Sakai R, Takahashi A, Takahira N, Uchiyama K, Yamamoto T, Uchida K, et al. Hammering force during cementless total hip arthroplasty and risk of microfracture. *Hip Int*. 2011;21(3):330–5. <https://doi.org/10.5301/HIP.2011.8408> PMID: 21698583
45. Arciola CR, Campoccia D, Montanaro L. Implant infections: adhesion, biofilm formation and immune evasion. *Nat Rev Microbiol*. 2018;16(7):397–409. <https://doi.org/10.1038/s41579-018-0019-y> PMID: 29720707
46. McNally M, Sousa R, Wouthuyzen-Bakker M, Chen AF, Soriano A, Vogely HC, et al. The EBJIS definition of periprosthetic joint infection. *Bone Joint J*. 2021;103-B(1):18–25. <https://doi.org/10.1302/0301-620X.103B1.BJJ-2020-1381.R1> PMID: 33380199
47. Craig MR, Poelstra KA, Sherrell JC, Kwon MS, Belzile EL, Brown TE. A novel total knee arthroplasty infection model in rabbits. *J Orthop Res*. 2005;23(5):1100–4. <https://doi.org/10.1016/j.orthres.2005.03.007> PMID: 15927441
48. Broekhuizen CAN, de Boer L, Schipper K, Jones CD, Quadir S, Vandenbroucke-Grauls CMJE, et al. *Staphylococcus epidermidis* is cleared from biomaterial implants but persists in peri-implant tissue in mice despite rifampicin/vancomycin treatment. *J Biomed Mater Res A*. 2008;85(2):498–505. <https://doi.org/10.1002/jbm.a.31528> PMID: 17729261
49. Broekhuizen CAN, de Boer L, Schipper K, Jones CD, Quadir S, Feldman RG, et al. Peri-implant tissue is an important niche for *Staphylococcus epidermidis* in experimental biomaterial-associated infection in mice. *Infect Immun*. 2007;75(3):1129–36. <https://doi.org/10.1128/IAI.01262-06> PMID: 17158900
50. Dreikausen L, Blender B, Trifunovic-Koenig M, Salm F, Bushuven S, Gerber B, et al. Analysis of microbial contamination during use and reprocessing of surgical instruments and sterile packaging systems. *PLoS One*. 2023;18(1):e0280595. <https://doi.org/10.1371/journal.pone.0280595> PMID: 36668667
51. Guarch-Pérez C, Riool M, de Boer L, Kloen P, Zaat SAJ. Bacterial reservoir in deeper skin is a potential source for surgical site and biomaterial-associated infections. *J Hosp Infect*. 2023;140:62–71. <https://doi.org/10.1016/j.jhin.2023.07.014> PMID: 37544367
52. Rakow A, Perka C, Trampuz A, Renz N. Origin and characteristics of haematogenous periprosthetic joint infection. *Clin Microbiol Infect*. 2019;25(7):845–50. <https://doi.org/10.1016/j.cmi.2018.10.010> PMID: 30678837
53. Pankey GA, Sabath LD. Clinical relevance of bacteriostatic versus bactericidal mechanisms of action in the treatment of Gram-positive bacterial infections. *Clin Infect Dis*. 2004;38(6):864–70. <https://doi.org/10.1086/381972> PMID: 14999632
54. Xia Y, Adibnia V, Shan C, Huang R, Qi W, He Z, et al. Synergy between Zwitterionic Polymers and Hyaluronic Acid Enhances Antifouling Performance. *Langmuir*. 2019;35(48):15535–42. <https://doi.org/10.1021/acs.langmuir.9b01876> PMID: 31478669
55. Chen X, Zhou J, Qian Y, Zhao L. Antibacterial coatings on orthopedic implants. *Mater Today Bio*. 2023;19:100586. <https://doi.org/10.1016/j.mtbio.2023.100586> PMID: 36896412
56. Hayakawa T, Yoshinari M, Kiba H, Yamamoto H, Nemoto K, Jansen JA. Trabecular bone response to surface roughened and calcium phosphate (Ca-P) coated titanium implants. *Biomaterials*. 2002;23(4):1025–31. [https://doi.org/10.1016/s0142-9612\(01\)00214-9](https://doi.org/10.1016/s0142-9612(01)00214-9) PMID: 11791905

57. Sul Y-T, Byon E, Jeong Y. Biomechanical measurements of calcium-incorporated oxidized implants in rabbit bone: effect of calcium surface chemistry of a novel implant. *Clin Implant Dent Relat Res*. 2004;6(2):101–10. <https://doi.org/10.1111/j.1708-8208.2004.tb00032.x> PMID: [15669710](#)
58. Breeding K, Jimbo R, Hayashi M, Xue Y, Mustafa K, Andersson M. The effect of hydroxyapatite nanocrystals on osseointegration of titanium implants: an in vivo rabbit study. *Int J Dent*. 2014;2014:171305. <https://doi.org/10.1155/2014/171305> PMID: [24563651](#)
59. Roberts WE, Smith RK, Zilberman Y, Mozsary PG, Smith RS. Osseous adaptation to continuous loading of rigid endosseous implants. *Am J Orthod*. 1984;86(2):95–111. [https://doi.org/10.1016/0002-9416\(84\)90301-4](https://doi.org/10.1016/0002-9416(84)90301-4) PMID: [6589962](#)
60. Slaets E, Carmeliet G, Naert I, Duyck J. Early cellular responses in cortical bone healing around unloaded titanium implants: an animal study. *J Periodontol*. 2006;77(6):1015–24. <https://doi.org/10.1902/jop.2006.050196> PMID: [16734577](#)
61. Hermida JC, Bergula A, Dimaano F, Hawkins M, Colwell CW Jr, D'Lima DD. An in vivo evaluation of bone response to three implant surfaces using a rabbit intramedullary rod model. *J Orthop Surg Res*. 2010;5:57. <https://doi.org/10.1186/1749-799X-5-57> PMID: [20712889](#)